

AD-A055 274

STANFORD UNIV CALIF EDWARD L GINZTON LAB

F/G 20/5

STUDIES OF TECHNIQUES FOR GENERATION OF VACUUM ULTRAVIOLET AND --ETC(U)

MAY 78 S E HARRIS

N00014-75-C-0576

UNCLASSIFIED

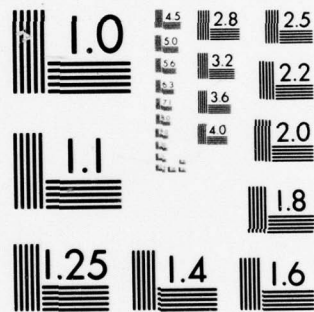
OL-2811

NL

| OF |  
AD  
A055274



END  
DATE  
FILMED  
7 -78  
DDC



MICROCOPY RESOLUTION TEST CHART  
NATIONAL BUREAU OF STANDARDS-1963-A

AD A 055274

FOR FURTHER TRAN  
A033778

STUDIES OF TECHNIQUES FOR GENERATION OF  
VACUUM ULTRAVIOLET AND SOFT X-RAY LASER RADIATION

Office of Naval Research

Contract N00014-75-C-0576

FINAL REPORT

for the period

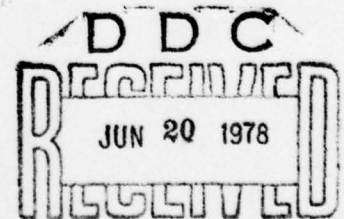
1 October 1976 - 30 April 1978

G. L. Report No. 2811

May 1978

Reproduction in whole or in part is permitted  
for any purpose of the United States Government.

Edward L. Ginzton Laboratory  
W. W. Hansen Laboratories of Physics  
Stanford University  
Stanford, California



AD No. \_\_\_\_\_  
DDC FILE COPY

DISTRIBUTION STATEMENT A  
Approved for public release  
Distribution Unlimited

78 06 13 053

UNCLASSIFIED

SECURITY CLASSIFICATION OF THIS PAGE (When Data Entered)

REPORT DOCUMENTATION PAGE		READ INSTRUCTIONS BEFORE COMPLETING FORM
1. REPORT NUMBER	2. GOVT ACCESSION NO.	3. RECIPIENT'S CATALOG NUMBER
4. TITLE (and Subtitle) STUDIES OF TECHNIQUES FOR GENERATION OF VACUUM ULTRAVIOLET AND SOFT X-RAY LASER RADIATION.		5. TYPE OF REPORT & PERIOD COVERED Final Report (covering period 1 Oct. 76 - 30 Apr 78
7. AUTHOR(s) S. Harris (and Staff)		6. PERFORMING ORG. REPORT NUMBER G.L. 2811
10. S.E. / HARRIS (9) Final rept. 1 Oct 76 - 30 Apr 78		8. CONTRACT OR GRANT NUMBER(s) N00014-75-C-0576
9. PERFORMING ORGANIZATION NAME AND ADDRESS Edward L. Ginzton Laboratory Stanford University Stanford, California 94305		10. PROGRAM ELEMENT, PROJECT, TASK AREA & WORK UNIT NUMBERS Proj. Ele. 121107
11. CONTROLLING OFFICE NAME AND ADDRESS Office of Naval Research Physics Program Office Arlington, VA 22217		12. REPORT DATE May 1978
14. MONITORING AGENCY NAME & ADDRESS (if different from Controlling Office)		13. NUMBER OF PAGES 36
		15. SECURITY CLASS. (of this report) UNCLASSIFIED
		15a. DECLASSIFICATION/DOWNGRADING SCHEDULE
16. DISTRIBUTION STATEMENT (of this Report)  Approved for public release; distribution unlimited		
17. DISTRIBUTION STATEMENT (of the abstract entered in Block 20, if different from Report)		
18. SUPPLEMENTARY NOTES		
19. KEY WORDS (Continue on reverse side if necessary and identify by block number)  Laser induced collisional processes      Mode-locked dye lasers Dipole-dipole process Charge exchange process		
20. ABSTRACT (Continue on reverse side if necessary and identify by block number)  This report describes theoretical and experimental work on two types of laser induced collisional processes. These are the dipole-dipole process and the charge exchange process. Using two synchronously pumped mode-locked dye lasers, a dipole-dipole cross section of $4 \times 10^{-14} \text{ cm}^2$ has been demonstrated in the Sr-Ca system. We also report theoretical progress in the areas of laser induced spin exchange collisions and collisionally induced Raman processes. Lasing and inversion on the $\text{Sr}^+$ resonance line at 4078 Å is also described. This first demonstration of the inversion of an ion with respect		

DD FORM 1 JAN 73 1473

EDITION OF 1 NOV 65 IS OBSOLETE  
S/N 0102-LF-014-6601UNCLASSIFIED  
SECURITY CLASSIFICATION OF THIS PAGE (When Data Entered)

409640

CL



UNCLASSIFIED

SECURITY CLASSIFICATION OF THIS PAGE (When Data Entered)

20. to its ground state has important implications for the construction of short wavelength lasers.

S/N 0102- LF- 014- 6601

SECURITY CLASSIFICATION OF THIS PAGE(When Data Entered)

# I. INTRODUCTION

TEN TO THE MINUS 14TH  
POWER 59 CM

↓  
This report describes theoretical and experimental work on two types of laser induced collisional processes. These are the dipole-dipole process and the charge exchange process. Using two synchronously pumped mode-locked dye lasers, a dipole-dipole cross section of  $4 \times 10^{-14} \text{ cm}^2$  has been demonstrated in the Sr-Ca system. We also report theoretical progress in the areas of laser induced spin exchange collisions and collisionally induced Raman processes. Lasing and inversion on the  $\text{Sr}^+$  resonance line at 4078 Å is also described. This first demonstration of the inversion of an ion with respect to its ground state has important implications for the construction of short wavelength lasers.

We note that portions of the work described in this report were jointly supported by other agencies.

ANGSTROM

REVISION BY	
DATE	DATE SIGNED <input checked="" type="checkbox"/>
END	DATE SIGNED <input type="checkbox"/>
UNCLASSIFIED	<input type="checkbox"/>
JUSTIFICATION	
BY	
DISTRIBUTION/AVAILABILITY CODES	
SI. AVAIL. CODE OR SPECIAL	
A	

## II. LASER INDUCED DIPOLE-DIPOLE COLLISIONS:

### LARGE CROSS SECTION REGIME

Large cross sections are essential for the rapid, and thus efficient, extraction of stored energy. Our numerical calculations of the laser induced collision process indicate that this interaction should achieve cross sections in excess of  $10^{-13} \text{ cm}^2$  before experiencing saturation.<sup>1</sup> The experiment described in this report demonstrates the large collision cross sections that are achievable through a laser induced interaction. The results further confirm the validity of the theory used to describe this effect.

The experiment requires a gaseous medium, a pumping laser to create the stored population, a transfer laser to induce the collision, and a detection system to monitor the energy transfer. The laser induced collision is linear in the applied field intensity below saturation and requires a transfer laser capable of producing  $10^9 \text{ W/cm}^2$  power density to induce a collision cross section of  $10^{-13} \text{ cm}^2$ . Figure 1 shows a schematic of the experimental set-up used in this experiment. An actively mode-locked Nd:YAG oscillator amplifier system provides a reproducible train of 100 psec pulses at  $1.06 \mu\text{m}$ , which is converted in KDP crystals to 355 nm. This train of pulses is then split to pump two separate dye lasers whose cavity lengths are adjusted to match that of the Nd:YAG oscillator. In this case, the dye lasers also produce a train of mode-locked pulses which can be tuned by adjusting the angle of the rear

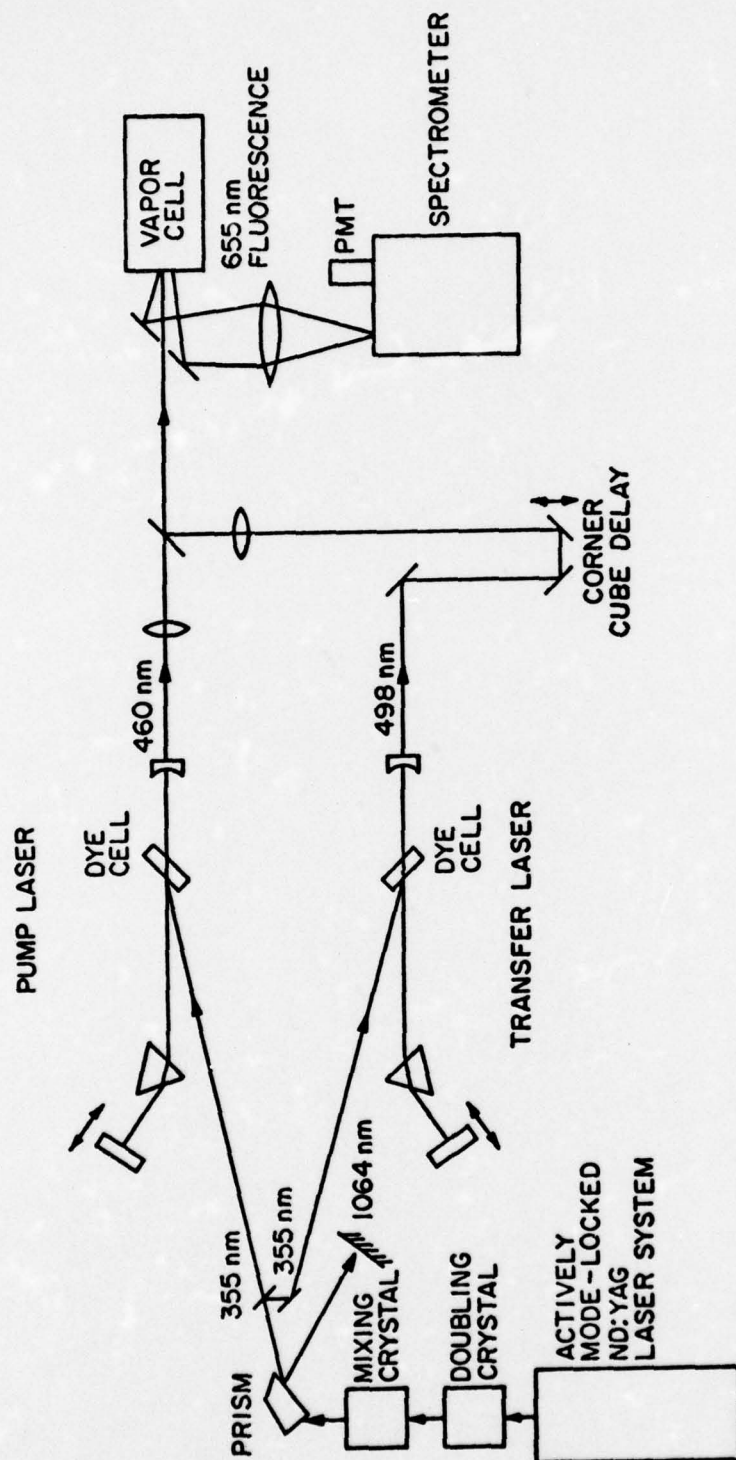


Fig. 1--Schematic of large cross section experiment.



mirrors.<sup>2</sup> This system produces an output power of several megawatts with a 40 psec pulsewidth. A key property of this system is that the pulses of both dye lasers are in exact time synchronism; a corner cube delay line can be used to give a precise and adjustable delay between the pump and transfer lasers. The outputs of the two lasers are combined and focused into the vapor cell. A spectrometer and photomultiplier are used to detect the fluorescence of the excited state population produced by the transfer process.

In this experiment, Sr and Ca were heated to 800°C providing ground state number densities near  $10^{16}$  atoms/cm<sup>3</sup>. The transfer beam was focused to an area of  $10^{-3}$  cm<sup>2</sup> providing a power density in the vapor cell of  $4 \times 10^8$  W/cm<sup>2</sup>. The stored population was measured by first applying a laser to transfer the population from the storage state to a higher state in the same atom, and then observing the fluorescence from that state. By taking the ratio of this fluorescence to the fluorescence from the final state in Ca from the laser induced collision, most geometric, calibration and loss factors are eliminated from the determination of the experimental cross section. This is illustrated by the following equation:

$$\sigma_{\text{exp}} = \frac{N_{\text{Ca}}^*}{N_{\text{Sr}}^*} \times \frac{1}{N_{\text{Ca}} \bar{V} \tau}$$

where  $\bar{V}$  = velocity and  $\tau$  = pulsewidth. The pump laser created a Sr excited state number density of  $10^{12}$  atoms/cm<sup>3</sup>.

The experimental cross section was determined to be  $4 \times 10^{-14}$  cm<sup>2</sup>. This is to be compared to the theoretical cross section of  $3 \times 10^{-14}$  cm<sup>2</sup>. The agreement is actually better than the systematic errors would predict.



The experiment illustrates that the laser induced collision can indeed be a strong effect and that our analytic model for this process is valid up to these signal levels.

References:

1. L. S. Goldberg and C. A. Moore, "Synchronous Mode-Locked Dye Lasers for Picosecond Spectroscopy and Nonlinear Mixing," in Laser Spectroscopy, S. Haroche, J. C. Pebay-Peyroula, T. W. Hansch, and S. E. Harris, eds. (New York: Springer-Verlag, 1975).
2. S. E. Harris and J. C. White, "Numerical Analysis of Laser Induced Inelastic Collisions," IEEE J. Quant. Elect. QE-13, 972 (December 1977).

### III. LASER INDUCED SPIN EXCHANGE COLLISIONS

In the area of laser induced collisions, attention has primarily been focused on the dipole-dipole collision. In order to transfer stored population using a dipole-dipole "switched" collision, two of the three pertinent states must have dipole matrix elements to the ground state. This eliminates most triplet states from consideration because they are usually very weakly coupled to the ground state. It is exactly this weak coupling which makes triplet states attractive for energy storage. To exploit the energy storing capability of the triplet manifold, the laser induced spin exchange collision was analytically evaluated.

The cross section for laser induced dipole-dipole collisions peaks for a transfer energy equal to the energy separation of the initial and final states when the atoms are fully separated. One might expect the electromagnetic absorption to increase in strength as the atoms approach each other. However, detailed analysis shows that the square of the effective interaction time varies inversely as the slope of the relative energy difference of the initial and final states and so increases as  $R^7$ , thus more than compensating for the  $1/R^6$  roll-off of the square of the dipole-dipole interaction.<sup>1</sup> When spin exchange collisions are considered, the interaction Hamiltonian no longer has the long range  $1/R^6$  dependence of the dipole-dipole interaction, but rather has an exponential roll-off. The square of the interaction time still varies as  $R^7$  and thus the exponential soon dominates with increasing  $R$  and the cross section maximizes

at a close atomic separation, producing a transfer energy which is shifted from the  $R = \infty$  energy separation.

The cross section is evaluated in the quasi-static regime under weak field conditions where:

$$\sigma_c = 2\pi R_x^2 P$$

$R_x$  is the curve crossing radius defined by the frequency of the applied field, and  $P$  is the probability of transfer.  $P$  is proportional to the square of the product of the interaction Hamiltonian and the effective interaction time:

$$P = \left| \frac{H'_{12} \Delta t}{\hbar} \right|^2$$

As noted previously, the square of the effective interaction time varies as  $R_x^7$ . Finally, the interaction Hamiltonian for spin exchange is evaluated as the Coulomb repulsion integral between the initial and intermediate states, and falls off exponentially with  $R_x$ . Hydrogen-like wave functions were used in this evaluation. The intermediate state is coupled by the applied field to the final state through the dipole matrix element between the two states.

This analytic treatment was applied to an experimental system consisting of excited state Ca (in triplet state) transferred to an upper triplet state in Sr. The result is:

$$\sigma_c = 6 \times 10^{-22} \frac{P}{A} \text{ cm}^2$$

where  $P/A$  is in  $W/cm^2$ . The maximum cross section approaches  $10^{-14} cm^2$ . This clearly shows that laser induced triplet-triplet energy exchange can be a process of significant strength.

Calculations predict that the peak cross section should occur within  $100 cm^{-1}$  of the  $R = \infty$  frequency and that the linewidth of the effect should be very broad, perhaps several hundred wavenumbers.

This may be a very promising future application of the laser induced interaction. Initial demonstration of this process will be challenging, however, because precise determination of the appropriate transfer frequency is more difficult than in the case of the  $R = \infty$  frequency of the dipole-dipole interaction.

#### References:

1. S. E. Harris, D. B. Lidow, R. W. Falcone, and J. F. Young, "Laser Induced Collisions," in Tunable Lasers and Applications, A Mooradian, T. Jaeger, and P. Stokseth, eds. (New York: Springer-Verlag, 1976).



#### IV. COLLISIONALLY INDUCED RAMAN EMISSION

A natural outgrowth of the laser induced dipole-dipole collision is a collisionally induced coherent Raman emission. Figure 2 illustrates such a process which could either be a Stokes or an anti-Stokes emission from an energy level in atom A to an energy level in atom B, thus potentially being used as an up-converter or down-converter. It is important to notice that the storage state need not be inverted with respect to its ground state to achieve stimulated Raman emission.

An analytic evaluation was made of the Raman process and the gain has the following functional form:

$$\alpha = \frac{\hbar \omega N_A^* N_B \pi}{\bar{V}} \left[ \left( \frac{\mu_1^A}{2\hbar \Delta \omega_A} \right)^2 E^2 \right] \left( \frac{2\mu_1^A \mu_2^B}{\hbar \rho_{Om}} \right)^2 \left[ \left( \frac{\mu_2^B}{2\hbar \Delta \omega_B} \right)^2 \frac{8\pi}{c} \right]$$

where

$\omega$  = frequency of the applied field

$\bar{V}$  = velocity

$\mu_1^A, \mu_2^A$  = s-p matrix elements of atom A

$\mu_1^B, \mu_2^B$  = s-p matrix elements of atom B

$\rho_{Om}$  = dephasing radius

$\Delta \omega_A$  = detuning in atom A

$\Delta \omega_B$  = detuning in atom B



# COHERENT RAMAN PROCESSES

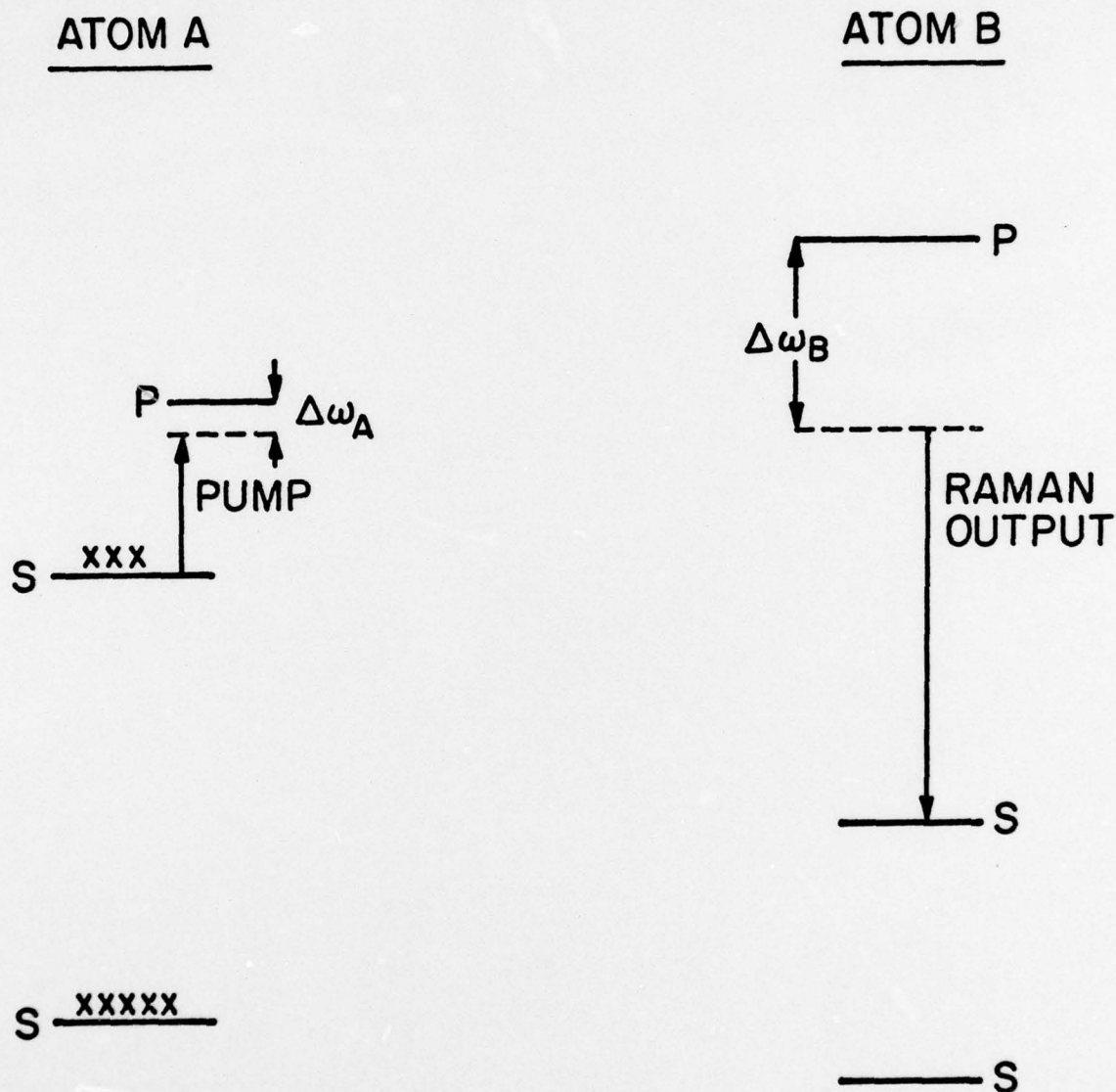


Fig. 2--In a coherent collisional Raman process gain is obtained at the Raman output frequency. Note that atom A need not be inverted, and that the frequency of the Raman output may be higher than that of the pumping frequency.

The gain saturates when the term  $(\mu_1^A / 2\hbar\Delta\omega_A)^2 E^2$  approaches 1/2. Thus, for maximum Raman gain in a given atomic system, the pump laser should be tuned to minimize  $\Delta\omega_B$  since the resulting large  $\Delta\omega_A$  (note that  $\Delta\omega_A + \Delta\omega_B = \text{constant} = \text{energy separation of the } p \text{ states}$ ) can be compensated for by increasing the pump field intensity.

The gain of the Raman system was then evaluated for decreasing  $\Delta\omega_B$ . In the development of the gain formula, the assumption that  $e^{j\Delta\omega_B t}$  is a more rapidly varying function of time than the dipole-dipole interaction Hamiltonian, proportional to  $1/R^3(t)$ , is made. As  $\Delta\omega_B$  becomes smaller than  $\bar{V}/P$  then  $1/R^3(t)$  is now the most rapidly varying term and this has the effect of replacing  $\rho_{Om}$  by  $\bar{V}/\Delta\omega_B$  in the previous formula, thus eliminating  $\Delta\omega_B$  from the formula. A physical interpretation of this phenomena can be realized by understanding that the  $p$  state in atom B is actually being shifted by the interaction during the collision and clearly when it shifts more than  $\Delta\omega_B$  during the interaction,  $\Delta\omega_B$  is no longer a relevant quantity. It should also be noted that there is no longer any explicit dephasing radius in the gain formula. This can be motivated in the following manner. Previous work has shown that the bulk of the switched interaction occurs near  $\rho_{Om}$ .<sup>1</sup> Then consider

$$\sigma = 2\pi\rho_{Om}^2 P$$

where

$$P = |H_{12}\Delta t/\hbar|^2 = \text{probability of transfer}$$

$$H_{12} = \text{dipole-dipole Hamiltonian proportional to } \rho_{Om}^{-3}/\Delta\omega_B'$$

$\Delta\omega'_B = \text{effective detuning from the } p \text{ state in atom B}$

$\Delta t = \text{effective interaction time proportional to } \rho_{Om}/\sqrt{V}$

Therefore,  $\sigma \propto \rho_{Om}^{-2}/\Delta\omega'_B$ , but if  $\Delta\omega_B$  is made so small that the detuning is determined by the shifting of the  $p$  state, the  $\Delta\omega'_B \propto \bar{V}/\rho_{Om}$  and the cross section has no explicit dependence on  $\rho_{Om}$ .

Therefore we find the very interesting result that the maximized Raman gain for small detunings in atom B is independent of the detuning in atom B and independent of the dephasing of the initial and final states. In the more complex case, where the  $p$  state of atom B is dominately dephased by other states in the system, then  $\rho_{Om}$  is replaced by a  $\rho'_{Om}$  calculated from these states and the maximized Raman gain is reduced.

#### References:

1. L. S. Goldberg and C. A. Moore, "Synchronous Mode-Locked Dye Lasers for Picosecond Spectroscopy and Nonlinear Mixing," in Laser Spectroscopy, S. Haroche, J. C. Pebay-Peyroula, T. W. Hansch, and S. E. Harris, eds. (New York: Springer-Verlag, 1975).

## V. INVERSION OF THE RESONANCE LINE OF $\text{Sr}^+$

We report the successful inversion of an ion by selective transfer of ground state atoms into excited ionic states. This is a technique which has significance for the production of VUV and x-ray lasers. The experiment also involves the use of a doubly excited electronic level. Doubly excited levels, particularly those above the continuum, may also play an important role in the construction of short wavelength lasers. A full description of this work has been published in the literature and is attached as Appendix A.



## V. INVERSION OF THE RESONANCE LINE OF $\text{Sr}^+$

We report the successful inversion of an ion by selective transfer of ground state atoms into excited ionic states. This is a technique which has significance for the production of VUV and x-ray lasers. The experiment also involves the use of a doubly excited electronic level. Doubly excited levels, particularly those above the continuum, may also play an important role in the construction of short wavelength lasers. A full description of this work has been published in the literature and is attached as Appendix A.



## VI. DEMONSTRATION OF LASER INDUCED CHARGE EXCHANGE COLLISIONS

The theoretical development and experimental demonstration in this laboratory of laser induced inelastic collisions between neutral atomic species<sup>1-4</sup> has led us to predict the existence of a similar collision phenomenon between ionic and neutral atomic species. It is expected that a highly endothermic charge exchange reaction having a very small cross section may be made to proceed with a large cross section by application of an intense photon field within a proper frequency bandwidth. The purpose of this project has been to experimentally demonstrate such a laser induced, or "switched", charge exchange reaction.

A particular type of laser induced charge exchange reaction is written as



An energy level diagram associated with this reaction is shown in Fig. 3. In the beginning of this project, a detailed theoretical examination was made of this reaction, and an expression for the cross section was derived. We found that

$$\sigma = \frac{2\pi^3 (R_x)^7 |\mu_{21}|^2 |H_{32}|^2 (P/A)}{n^3 e^2 c \bar{V} (\Delta\omega)^2 |\alpha(A^*) - \alpha(B)|} \quad (2)$$

where  $R_x$  is the curve-crossing distance (the inter-nuclear separation between the A and B species such that the energy curves associated with

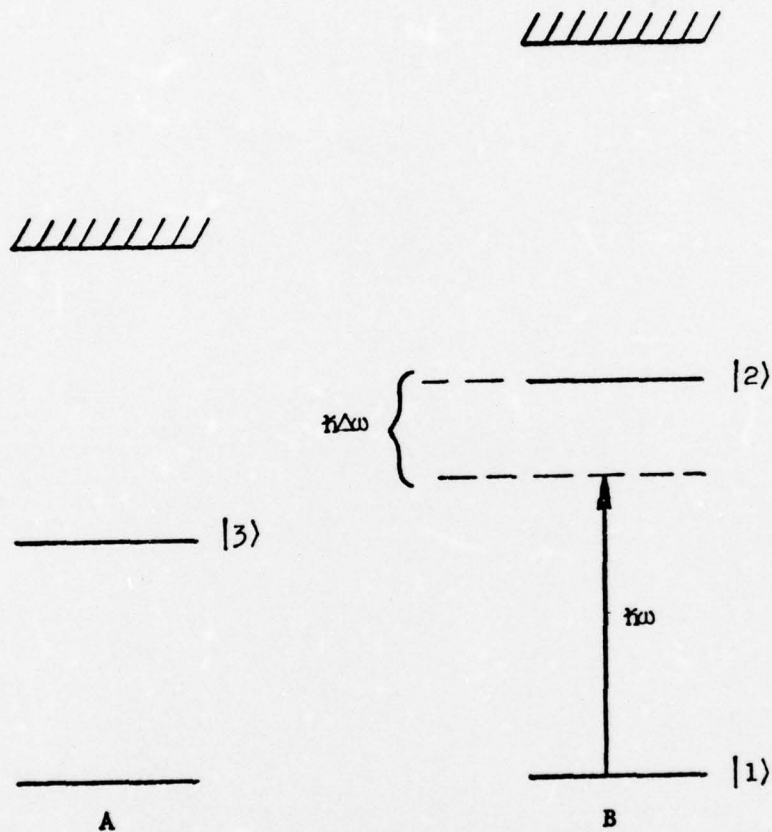
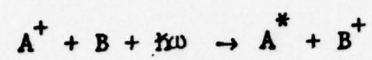
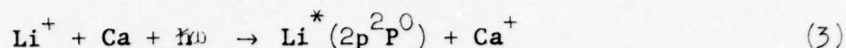


Fig. 3--Energy level diagram for switched charge exchange reaction.

the left and right hand sides of Eq. (1) cross; this distance is determined by the frequency of the applied photon field),  $\mu_{21}$  is the matrix element of the dipole moment between states  $|1\rangle$  and  $|2\rangle$  of atom B,  $H_{32}$  is the matrix element of the charge exchange Hamiltonian between state  $|2\rangle$  of atom B and state  $|3\rangle$  of atom A,  $(P/A)$  is the power density of the applied photon field,  $\bar{V}$  is the mean relative speed between the A and B species,  $\Delta\omega$  is the detuning of the applied photon field with respect to state  $|2\rangle$  of atom B, and  $\alpha(A^*)$  and  $\alpha(B)$  are the static polarizabilities of atom A in state  $|3\rangle$  and atom B in state  $|1\rangle$ , respectively.

Following the theoretical development mentioned above, a search was made for the particular atomic species which hold the most promise for an experimental demonstration of the switched charge exchange effect. An "ideal" system is characterized by the following qualities: the polarizability of B is greater than the polarizability of  $A^*$ , so that a natural curve-crossing does not exist and the product species have enough energy to separate; the applied exchange radiation is in the visible where tunability and moderate pulse energies are available; and  $\sigma/(P/A)$  is large enough such that available energy in the exchange radiation pulse is large enough to create a signal arising from the fluorescence of  $A^*$  excited neutrals which is greater than the noise level arising from recombination of  $A^+$  ions with electrons. With these requirements in mind, reactions among the alkali metals and Ca, Sr, and Ba of the alkaline-earth metals were considered. Static polarizabilities of the ground and first excited states of each of these atoms were computed. Of these metal-metal systems, the system which best met all of the above-mentioned requirements

was found to be



The energy level diagram associated with this reaction is shown in Fig. 4.

Calculations of theoretical values for  $\sigma/(P/A)$  for the Li-Ca switched charge exchange system were carried out and are presented in Table 1. The values for  $\text{H}_{32}$  were obtained from an expression derived by Olson.<sup>5</sup> With exchange radiation at 4718 Å and a power density of  $5 \times 10^6 \text{ W-cm}^{-2}$ , a cross section of  $10^{-16} \text{ cm}^2$  is expected.

The experimental set-up which has been constructed to examine the Li-Ca switched charge exchange system is shown in Fig. 5. The Li and Ca vapors are produced in a heat pipe oven. The Li is photoionized by a pulse of 2128 Å radiation. 2128 Å is the fifth harmonic of Nd:YAG laser radiation at 1.06 μ and is generated via nonlinear optical processes in crystals. These processes consist of the doubling of 1.06 μ to produce 5320 Å, the doubling of 5320 Å to produce 2660 Å, and finally the mixing of 2660 Å and 1.06 μ to produce 2128 Å. An unstable resonator Nd:YAG laser is used to produce the 1.06 μ beam. The 5320 Å and 2660 Å crystals are operated at room temperature, whereas the 2128 Å crystal is cooled to -40°C.<sup>6</sup> The exchange radiation is produced by a flashlamp pumped dye laser. The signal at 6708 Å resulting from the fluorescence of  $\text{Li}^*(2p^2P^0)$  is observed with a spectrometer and photomultiplier tube.

Prior to the construction of the experimental apparatus described above, calculations to determine expected signal levels and signal-to-noise ratios were made. At 1000°K, the Li and Ca number densities are  $7 \times 10^{15} \text{ cm}^{-3}$  and  $10^{15} \text{ cm}^{-3}$ , respectively.<sup>7</sup> For a  $\text{Li}^+$  ion density of  $10^{12} \text{ cm}^{-3}$ , and a switched



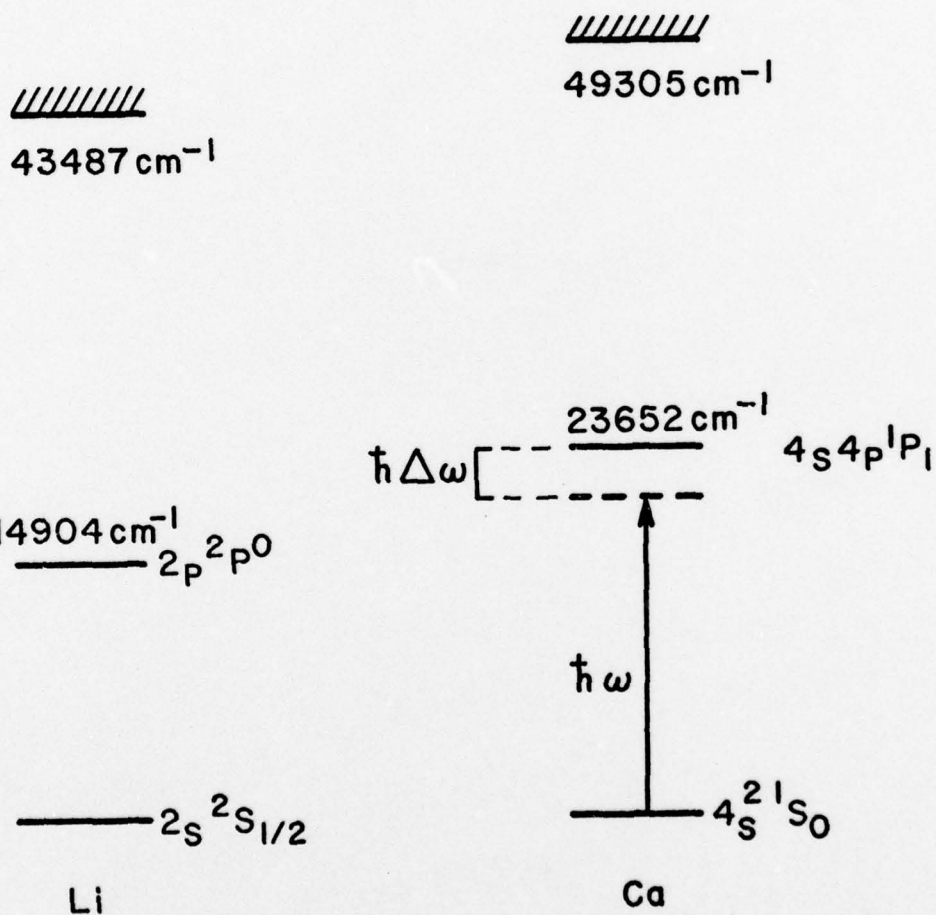


Fig. 4--Energy level diagram for switched charge exchange reaction described by Eq. (3).



Table 1  
Theoretical Values of Collision Cross Section  
for Switched Charge Exchange System  
Described by Eq. (3)

Induced Curve-Crossing Distance	Exchange Radiation	$\sigma/(P/A)$
5 Å	4718 Å	$2.0 \times 10^{-23} \text{ cm}^4 \text{ -W}^{-1}$
7 Å	4797 Å	$3.2 \times 10^{-24} \text{ cm}^4 \text{ -W}^{-1}$
10 Å	4819 Å	$2.8 \times 10^{-25} \text{ cm}^4 \text{ -W}^{-1}$

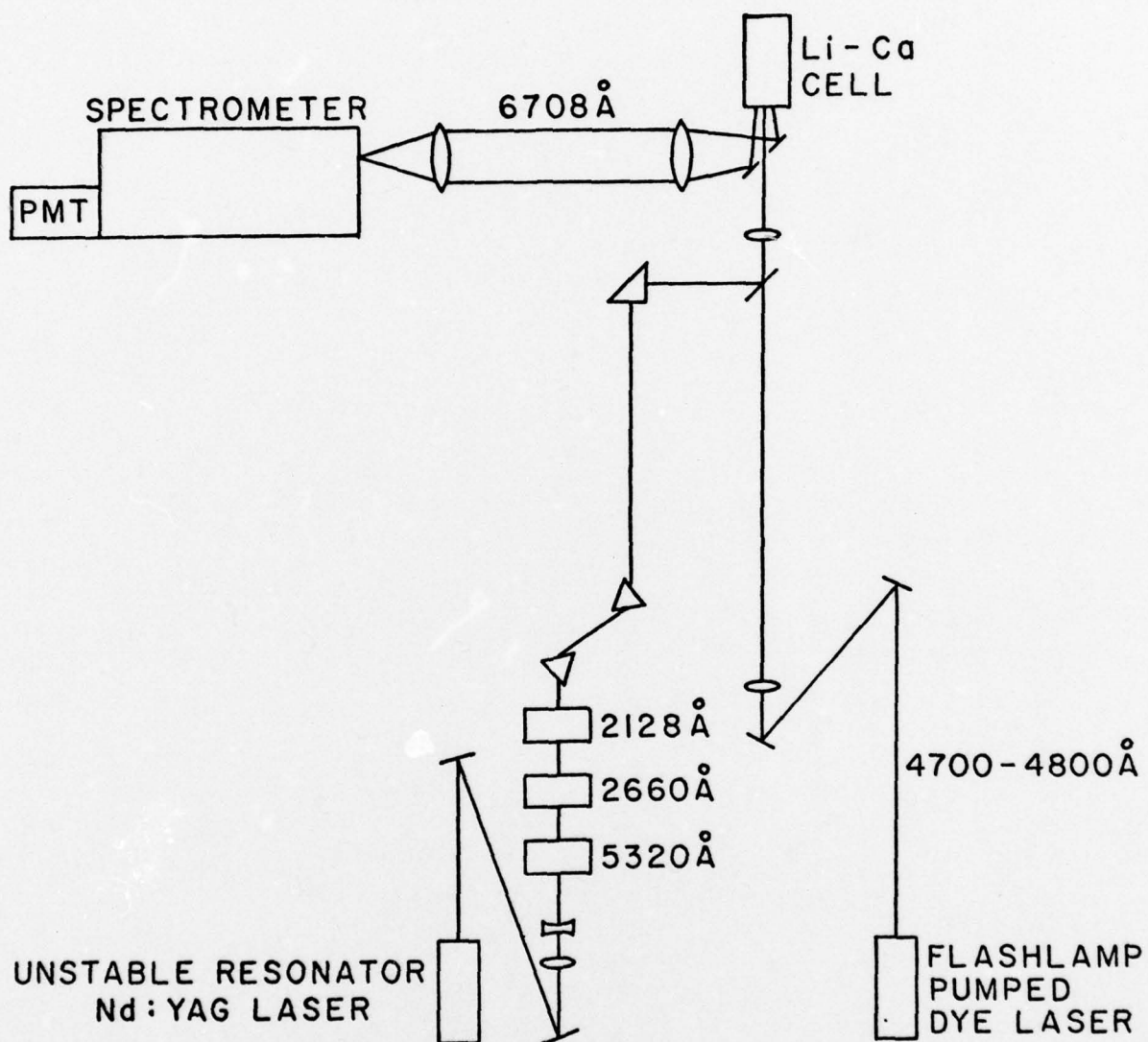


Fig. 5--Experimental set-up to observe Li-Ca switched charge exchange collision.

charge exchange cross section of  $10^{-16} \text{ cm}^3$ , we expect to create  $5 \times 10^7$  photons within the cell from the switched charge exchange effect. Based on recombination rate constants given by Bates,<sup>8</sup> we expect  $5 \times 10^3$  photons within the cell from recombination noise. This yields a theoretical signal-to-noise ratio of  $10^4$ .

After the construction of the apparatus necessary to examine the Li-Ca switched charge exchange reactions, we conducted some control experiments in which we injected 2128 Å photoionizing radiation into the heat pipe oven loaded with Li only in order to measure actual noise levels. These experiments led to surprising results. Basically, it was discovered that photons resulting from the fluorescence of  $\text{Li}^*$  excited states decayed at a rate which exhibited dependencies uncharacteristic of a recombination process, and that the noise level was much larger than predicted. Some experimental results are presented in Table 2; theoretical values for the collisional-radiative recombination time constants at electron temperature and densities comparable to that produced experimentally are presented in Table 3. It is apparent from Table 2 that the rate of decay of fluorescence from a  $\text{Li}^*$  excited state was independent of the electron density created by the 2128 Å photoionizing pulse. This is incongruent with a recombination process since the rate of formation of excited state species via recombination is dependent on the electron density, as exhibited in Table 3. It was also determined that although the rate of decay of fluorescent photons did not depend on the electron density, it did depend linearly on the neutral Li density. These surprising dependencies have led us to believe that the time constants which were measured are associated with electron cool-down rather than recombination.<sup>9</sup> The major thrust of these

Table 2  
Some Experimental Results

Neutral Li Density	2128 Å Energy Injected Into Cell	Ion and Electron Density Created	Time Constant for Decay of 6708 Å Radiation
$1.2 \times 10^{16} \text{ cm}^{-3}$	275 $\mu\text{J}$	$1.1 \times 10^{15} \text{ cm}^{-3}$	8 $\mu\text{sec}$
	15 $\mu\text{J}$	$6.0 \times 10^{13} \text{ cm}^{-3}$	
	0.6 $\mu\text{J}$	$2.4 \times 10^{12} \text{ cm}^{-3}$	

Table 3  
Theoretical Values for Collisional-Radiative  
Recombination Time Constant (After Ref. 8)

Electron Density*	Time Constant
$10^{15} \text{ cm}^{-3}$	$3.7 \times 10^{-6} \text{ sec}$
$10^{14} \text{ cm}^{-3}$	$2.0 \times 10^{-4} \text{ sec}$
$10^{12} \text{ cm}^{-3}$	$2.3 \times 10^{-1} \text{ sec}$

\* Electron temperature is 4000°K.



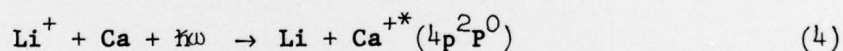
control experiments, however, was to reduce our expected signal-to-noise ratio from  $10^4$  to 5.

After the control experiments described above, an attempt was made to experimentally observe the actual Li-Ca switched charge exchange reaction. This attempt proved unsuccessful. The pertinent experimental procedures and parameters were as follows: a pulse of 2128 Å photoionizing radiation, and a pulse of 4720 Å exchange radiation were spatially and temporally overlapped and injected into the heat pipe oven containing Li and Ca at 773°C. The 2128 Å pulse energy was  $10^{-7}$  J, and the 4720 Å pulse energy was  $10^{-3}$  J; both pulses were focused to an area of  $3 \times 10^{-4}$  cm<sup>2</sup> at the center of the oven, and the active zone length was 10 cm. The Li and Ca number densities were  $10^{16}$  cm<sup>-3</sup> and  $2 \times 10^{15}$  cm<sup>-3</sup>, respectively. For these parameters, the switched charge exchange effect was expected to yield  $4 \times 10^3$  photons at 6708 Å at the detector. The actual signal level observed was  $4 \times 10^5$  photons. This signal vanished when the 4720 Å beam was blocked, but remained at the same level when the 2128 Å beam was blocked. This signal also remained at the same level as the exchange radiation was tuned from 4700 Å to 4750 Å.

The physical mechanism which produced the large noise level described above is most probably the absorption of the exchange laser radiation by Li<sub>2</sub> dimers followed by dissociation of the excited state dimers into Li and Li<sup>\*</sup>(2p<sup>2</sup>P<sup>0</sup>). We knew for some time that the exchange radiation fell within an absorption band of the Li<sub>2</sub> dimer,<sup>10,11</sup> although we could not find a cross section for absorption reported in the literature, and thereby were not able to calculate the amount of such absorption. Based on our experimental results, it is now apparent that absorption is strong. The pertinent

transition in the  $\text{Li}_2$  dimer is the  $X^1\Sigma_g^+ \rightarrow B^1\Pi_u$  transition as shown in Fig. 6. It is evident from Fig. 6 that the minimum of the  $B^1\Pi_u$  state lies approximately  $3000 \text{ cm}^{-1}$  below the energy associated with the infinitely separated  $\text{Li}$  and  $\text{Li}^*(2p^2P^0)$  atoms. If it is assumed that the exchange radiation saturated the  $X^1\Sigma_g^+ \rightarrow B^1\Pi_u$  transition, that all  $\text{Li}_2^*(B^1\Pi_u)$  excited state dimers with kinetic energy greater than  $3000 \text{ cm}^{-1}$  emerged as  $\text{Li}$  and  $\text{Li}^*(2p^2P^0)$  atoms, and that all  $\text{Li}^*(2p^2P^0)$  excited state atoms formed emitted a  $6708 \text{ \AA}$  photon, then it is expected that  $5 \times 10^5$  photons would enter the detector. This number compares well with the  $4 \times 10^5$  photons observed.

The large noise levels observed in the attempt to experimentally demonstrate the Li-Ca switched charge exchange collision described by Eq. (3) led us to halt work on this system. An effort was made, however, to find a switched charge exchange system which avoids the noise sources associated with the previous experiment. A system which was proposed is given by Eq. (4):



In this system, exchange occurs into an excited state of the  $\text{Ca}^+$  ion; as such, there is no noise arising from recombination. A theoretical analysis of this system was conducted, and the results are presented in Table 4. The disadvantages of this system relative to the first system include the lower values for  $\sigma/(P/A)$ , and the requirement of UV radiation to induce the exchange. In spite of these disadvantages, calculations indicate that a signal of  $1.5 \times 10^3$  photons arising from the fluorescence of  $\text{Ca}^{+*}$  ions at  $3934 \text{ \AA}$  may be expected at the detector. We conducted some control

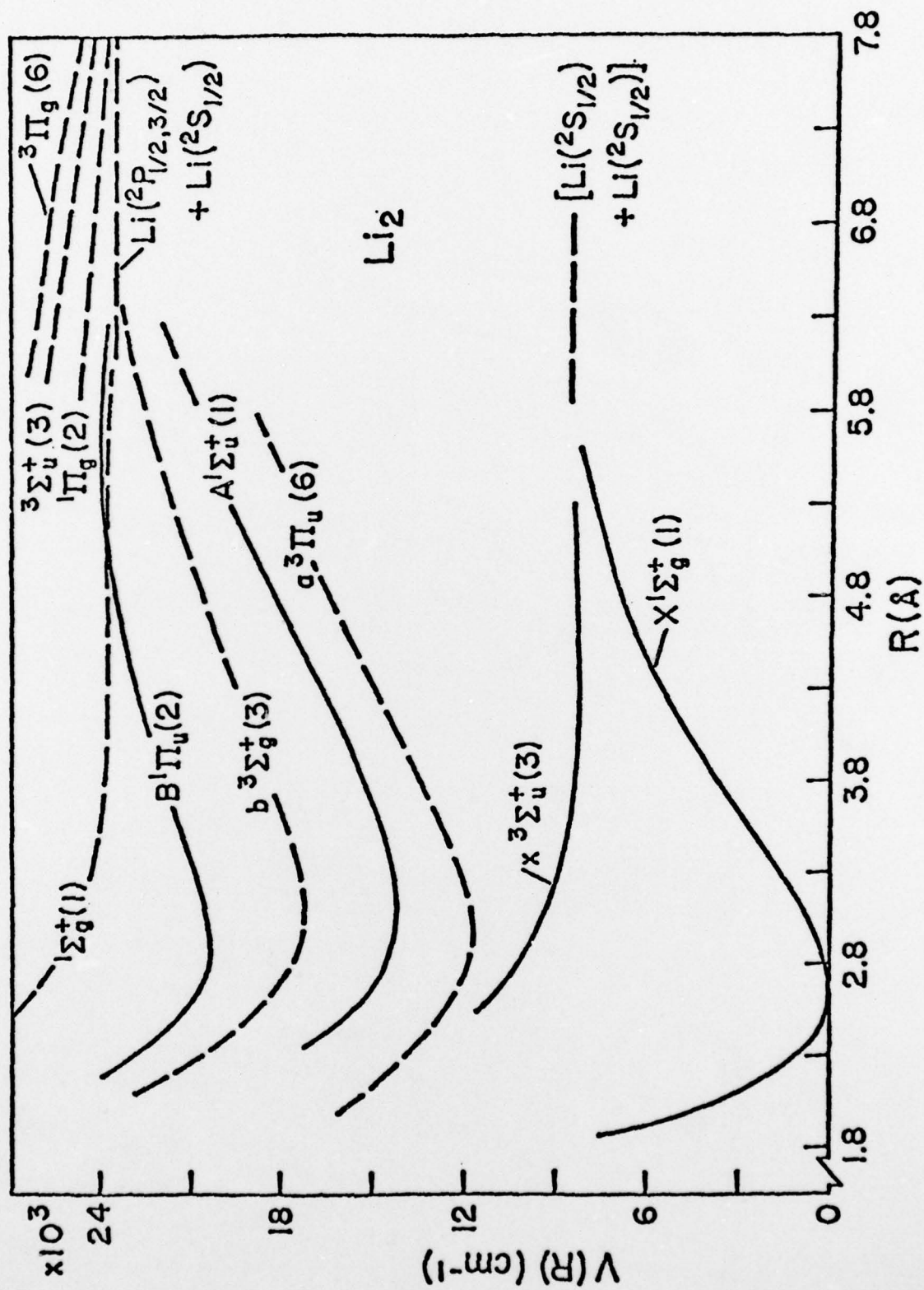


Fig. 6--Lowest electronic states of  $\text{Li}_2$  (after Ref. 11).

Table 4  
Theoretical Values of Collision Cross Section  
for Switched Charge Exchange System  
Described by Eq. (4)

Induced Curve-Crossing Distance	Exchange Radiation	$\sigma/(P/A)$
5 Å	3237 Å	$5.6 \times 10^{-27} \text{ cm}^4 \text{ -W}^{-1}$
7 Å	3228 Å	$3.2 \times 10^{-27} \text{ cm}^4 \text{ -W}^{-1}$
10 Å	3226 Å	$1.9 \times 10^{-28} \text{ cm}^4 \text{ -W}^{-1}$



experiments in which we injected 2128 Å photoionizing radiation into a cell containing Li only in an effort to measure noise level at 3934 Å. Surprisingly, we measured a noise level slightly greater than the expected signal level. It has been determined that this noise arises from a broadband transition in Li centered at 3915 Å, the Li<sup>\*</sup> excited state atoms being produced by recombination of Li<sup>+</sup> ions with electrons (the slit widths of the spectrometer were set such that the detection system had a bandwidth of 5 Å; noise at 3934 Å was observed because the transition in Li centered at 3915 Å is very broadband).<sup>12</sup>

In summary, much theoretical and experimental work has been conducted in the past year in an effort to experimentally demonstrate laser induced charge exchange collisions. The experimental work has uncovered noise sources much larger than anticipated theoretically; as a result, the efforts to observe switched charge exchange collisions have proven unsuccessful. The project has been discontinued for the present.

This project was jointly supported by the Air Force Rome Air Development Center under Contract F19628-77-C-0072.

#### References:

1. D. B. Lidow, R. W. Falcone, J. F. Young, and S. E. Harris, "Inelastic Collision Induced by Intense Optical Radiation," *Phys. Rev. Lett.* **36**, 462 (March 1976). [Erratum: *Phys. Rev. Lett.* **37**, 1590 (December 1976)].
2. S. E. Harris, D. B. Lidow, R. W. Falcone, and J. F. Young, "Laser Induced Collisions," in Tunable Lasers and Applications, A. Mooradian, T. Jaeger, and P. Stokseth, eds. (New York: Springer-Verlag, 1976).

3. R. W. Falcone, W. R. Green, J. C. White, J. F. Young, and S. E. Harris, "Observation of Laser Induced Inelastic Collisions," Phys. Rev. A 15, 1333 (March 1977).
4. S. E. Harris and J. C. White, "Numerical Analysis of Laser Induced Inelastic Collisions," IEEE J. Quant. Elect. QE-13, 972 (December 1977).
5. R. E. Olson, F. T. Smith, and E. Bauer, "Estimation of the Coupling Matrix Elements for One-Electron Transfer Systems," Appl. Optics 10, 1848 (August 1971).
6. G. A. Massey, "Efficient Upconversion of Long-Wavelength UV Light Into the 200-235 nm Band," Appl. Phys. Lett. 24, 371 (April 1974).
7. A. N. Nesmeyanov, Vapor Pressures of the Chemical Elements (New York: Elsevier Publishing Co., 1963), pp. 444-446.
8. D. R. Bates, ed., Atomic and Molecular Processes (New York: Academic Press, 1962), p. 257.
9. While Li atoms are ionized by the 2128 Å radiation, the ejected electrons have a temperature of 5000°K. As the electrons cool, the recombination rates become much greater. As such, the time constant for decay of fluorescence may be that associated with electron cool-down. Such a process is independent of electron density, and depends linearly on the neutral Li density. Calculations of electron cool-down times compare very well with the measured time constants. This explanation cannot be given full confidence, however, since certain experimental results still do not fit: at the low ion density of  $10^{12} \text{ cm}^{-3}$ , the measured

fluorescence decay time constant is much smaller than the theoretical recombination time constant at the ambient cell temperature. The electron cool-down explanation can only be correct if the actual values for recombination rates at low electron temperature and densities are considerably larger than the theoretical rates.

10. R. B. W. Pearse and A. G. Gaydon, The Identification of Molecular Spectra (New York: Halsted Press, 1976).
11. G. York and A. Gallagher, "High Power Gas Lasers Based on Alkali-Dimer A-X Band Radiation," Joint Institute for Laboratory Astrophysics Report No. 114 (15 October 1974).
12. G. R. Harrison, Massachusetts Institute of Technology Wavelength Tables (Cambridge: The MIT Press, 1969).

## APPENDIX A

### INVERSION OF THE RESONANCE LINE OF $\text{Sr}^+$ PRODUCED BY OPTICALLY PUMPING $\text{Sr}$ ATOMS<sup>\*</sup>

by

W. R. Green<sup>†</sup> and R. W. Falcone

Edward L. Ginzton Laboratory  
W. W. Hansen Laboratories of Physics  
Stanford University  
Stanford, California 94305

## ABSTRACT

We report inversion and lasing on the optically pumped resonance line of  $\text{Sr}^+$ . A mode locked frequency doubled dye laser was tuned to excite the dipole allowed two-electron transition  $5s^2\ ^1S_0 - 4d5p\ ^3P_1^0$  in  $\text{Sr}$  vapor. The same laser then ionized the excited atoms, selectively producing ions in the  $\text{Sr}^+\ 5p\ ^2P_{3/2}^0$  excited level. The inversion density with respect to the  $\text{Sr}^+$  ground level was approximately  $10^{13}\ \text{cm}^{-3}$ .

---

<sup>\*</sup>Work jointly supported by the National Aeronautics and Space Administration under Contract NGL-05-020-103 and the Office of Naval Research Contract No. N00014-75-C-0576.

<sup>†</sup>W. R. Green gratefully acknowledges support from the Fannie and John K. Hertz Foundation.



# INVERSION OF THE RESONANCE LINE OF $\text{Sr}^+$ PRODUCED

BY OPTICALLY PUMPING  $\text{Sr}$  ATOMS

by

W. R. Green and R. W. Falcone

Edward L. Ginzton Laboratory  
W. W. Hansen Laboratories of Physics  
Stanford University  
Stanford, California 94305

This Letter describes an experiment which demonstrates the selective production of excited state ions by optical absorption from neutrals. An inversion on the resonance line of  $\text{Sr}^+$  was produced by laser excitation of a two-electron transition, followed by ionization of one of the excited electrons by the same laser.

Figure 1 is an energy level diagram of the states of  $\text{Sr}$  pertinent to our experiment. A pulsed, mode locked laser operating at  $2680 \text{ \AA}$  was used to excite atoms from the  $\text{Sr } 5s^2 \text{ } ^1\text{S}_0$  ground level to  $\text{Sr } 4d5p^3 \text{ } ^3\text{P}_1^0$ . Although this is a two-electron transition between the singlet and triplet manifolds it has significant oscillator strength, about  $10^{-3}$ .<sup>1</sup> The same laser then ionized the excited atoms producing excited ions in the  $\text{Sr}^+ 5p^2 \text{ } ^3\text{P}_{3/2}^0$  level. This second step, into the continuum, was selective in producing excited ions as evidenced by lasing on the  $\text{Sr}^+ 5p^2 \text{ } ^3\text{P}_{3/2}^0 - 5s^2 \text{ } ^2\text{S}_{1/2}$  transition at  $4078 \text{ \AA}$ .

The selectivity of the ionization process can be understood by considering the configuration of the  $4d5p^3 \text{ } ^3\text{P}_1^0$  state as a composite addition of the core and the two valence electrons of  $\text{Sr}$  in separate orbitals: the  $4d$  and  $5p$ . Thus, if one of the electrons makes a transition to the continuum by

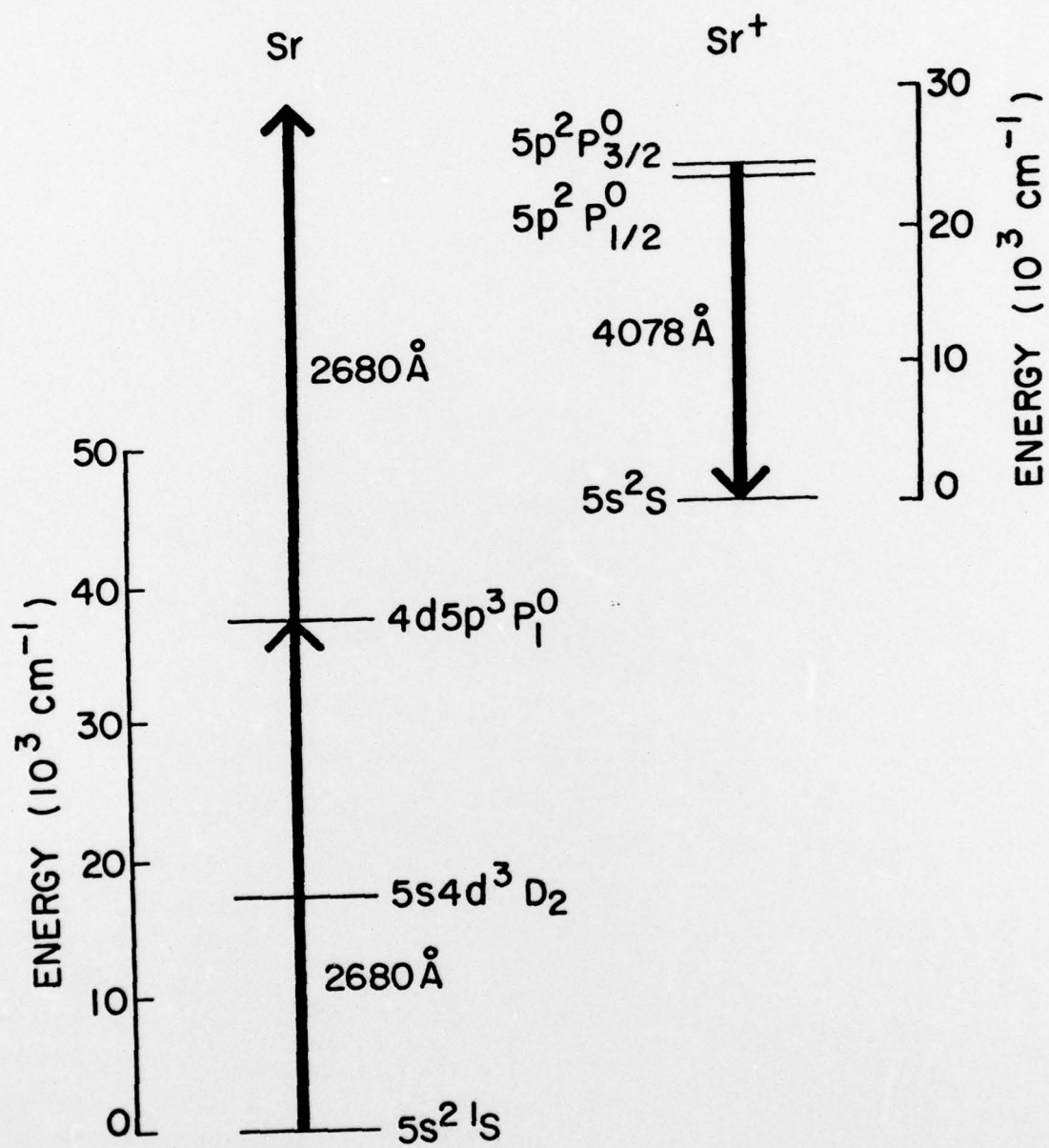


Fig. 1--Energy level diagram of Sr and Sr<sup>+</sup>.

the absorption of a photon, there will be a high probability that the final configuration of the ion will be that of the unaltered  $4p^6$  core plus an electron in either the excited  $4d$  or  $5p$  orbital. The wavelength of the ionizing radiation is not critical so long as it is above the bandhead because the absorption cross section into the continuum falls very slowly with increasing energy. In our experiment the  $2680 \text{ \AA}$  radiation is approximately  $4000 \text{ cm}^{-1}$  above the bandhead for the continuum state  $\text{Sr}^+ 5p^2 P_{3/2}^0 +$  electron.

The  $2680 \text{ \AA}$  pump beam was generated by frequency doubling the output of a synchronously pumped mode locked dye laser<sup>2</sup> in a KDP crystal. The dye laser was pumped by the third harmonic of a  $1.06 \text{ }\mu\text{m}$  mode locked pulse train consisting of 13 pulses, each 100 psec long, generated in an actively mode locked Nd:YAG laser.<sup>3</sup> The doubled dye laser output train had a total energy of 100  $\mu\text{J}$  in six pulses with a  $1.5 \text{ \AA}$  bandwidth and was focused to an area of  $10^{-5} \text{ cm}^2$  over a length of approximately 0.25 cm in a heat pipe type cell containing Sr vapor. The cell was operated at  $800^\circ\text{C}$  which provided a metal vapor density between  $10^{16}$  and  $10^{17}$  atoms/cc. Argon at a pressure of 100 torr was used as a buffer gas to prevent metal vapor condensation on the cell windows.

When the pump laser was tuned to  $2680 \text{ \AA}$  we observed fluorescence at both wavelengths of the  $5p$ - $5s$  ion resonance line doublet. Figure 2 shows the output energy as a function of pump power. When the pump energy was increased to 70  $\mu\text{J}$  the radiation at  $4078 \text{ \AA}$  from the  $5p^2 P_{3/2}^0 - 5s^2 S_{1/2}$  transition exhibited a rapid increase in output intensity for small changes in pump power indicating laser action. The other transition from the  $5p$  doublet at  $4216 \text{ \AA}$ ,  $5p^2 P_{1/2}^0 - 5s^2 S_{1/2}$ , did not exhibit lasing as indicated in the figure. The fluorescent output at  $4216 \text{ \AA}$  indicated approximately half as much population in the  $^2P_{1/2}$  state compared with the  $^2P_{3/2}$  state.

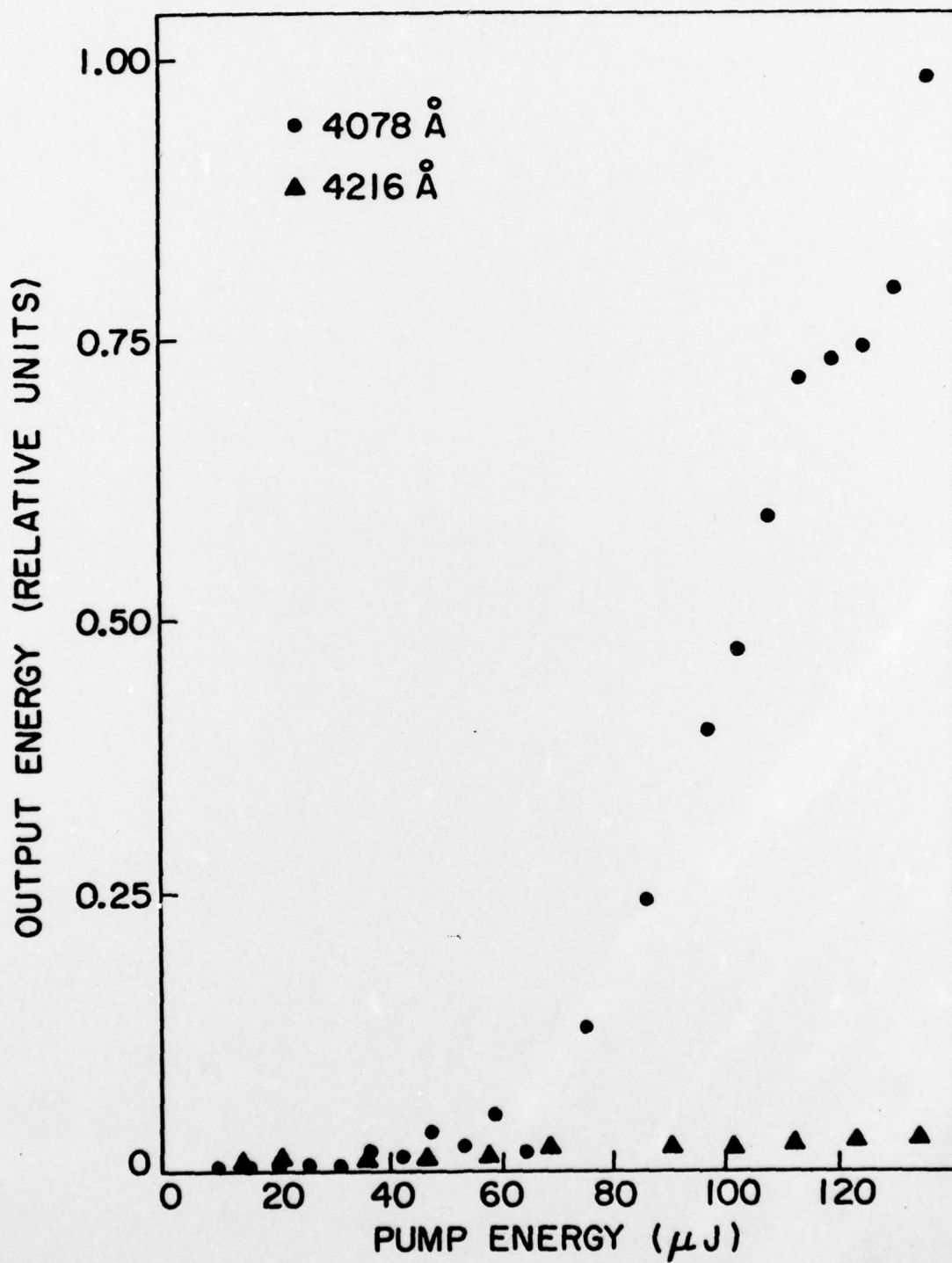


Fig. 2--Output energy of  $\text{Sr}^+$  doublet lines as a function of pump energy.



Spatial collimation of the radiation at  $4078 \text{ \AA}$  was verified by placing an aperture between the cell and detector. The aperture had no effect on collected intensity from the lasing transition yet it reduced the signal from the fluorescing transition at  $4216 \text{ \AA}$  by 80%.

The output energy of the lasing transition was approximately  $2 \times 10^{-11} \text{ J}$ , indicating an ionic inversion density of  $10^{13} \text{ cm}^{-3}$ . Lasing was most consistent when the pump laser was detuned slightly (less than  $2 \text{ \AA}$ ) from the  $4d5p^3P_1^0$  state, probably due to a trade-off between excited state population of this state, pump depletion, and beam distortion due to self-focusing effects. Because the pump beam intensity was near  $10^{10} \text{ W/cm}^2$ , multiphoton ionization of the ground state atoms must be considered as a source of ground state ions.

We also observed lasing at  $5239 \text{ \AA}$  in the neutral species from the intermediate two-electron state  $4d5p^3P_1^0$  to the  $5s4d^3D_2$  state. The  $5 \times 10^{-8} \text{ J}$  output energy of this beam implies that the  $5s^2 1S_0 - 4d5p^3P_1^0$  transition was very nearly saturated.

This experiment has demonstrated the selective production of excited state ions by optical absorption from neutrals. These results bear on the construction of VUV and x-ray lasers; many of the proposed methods for making such lasers depend on the selective production of excited state ions.<sup>4</sup> We have also shown that an atom can be selectively ionized into an excited state ion from a doubly excited configuration.

The authors gratefully acknowledge helpful discussions with S. E. Harris and J. F. Young.

## REFERENCES

1. The oscillator strength for this transition was estimated from a cw absorption measurement.
2. L. S. Goldberg and C. A. Moore, "Synchronously Mode-Locked Dye Lasers for Picosecond Spectroscopy and Nonlinear Mixing," in Laser Spectroscopy, R. G. Brewer and A. Mooradian, eds. (New York: Plenum Publishing Corp., 1974).
3. D. J. Kuizenga, D. W. Phillion, Terje Lund, and A. E. Siegman, "Simultaneous Q-Switching and Mode-Locking in the CW Nd:YAG Laser," Opt. Comm. 9, 221 (November 1973).
4. M. A. Duguay and P. M. Rentzepis, "Some Approaches to Vacuum UV and X-Ray Lasers," Appl. Phys. Lett. 10, 350 (1967).